Inorganic Chemistry

Communication

pubs.acs.org/IC

A Homologous Series of Cobalt, Rhodium, and Iridium Metalloradicals

Ayumi Takaoka and Jonas C. Peters*

Division of Chemistry and Chemical Engineering, California Institute of Technology, Pasadena, California 91125, United States

Supporting Information

ABSTRACT: We herein present a series of d^7 trimethylphosphine complexes of group 9 metals that are chelated by the tripodal tetradentate tris(phosphino)silyl ligand $[SiP^{iPr}_3]H$ ($[SiP^{iPr}_3] = (2\text{-}iPr_2PC_6H_4)_3Si^-$). Both electron paramagnetic resonance (EPR) simulations and density functional theory (DFT) calculations indicate largely metalloradical character. These complexes provide a rare opportunity to compare the properties between the low-valent metalloradicals of the second- and third-row transition metals with the corresponding first-row analogues.

Low-valent metalloradicals of the second- and third-row late transition metals are, in general, reactive species that have often necessitated in situ characterization.[1] There are a small number of well-defined examples of these $S = {}^1/_2$ metal-centered radicals, however, that point to their interesting spectroscopic properties and reactivity patterns.[1,2] Wayland's classic studies on rhodium(II) porphyrin complexes nicely illustrate the latter point.[3] The relative instability of these second- and third-row metalloradicals in comparison with their first-row congeners constitutes an interesting dichotomy in the chemistry of late transition metals.[4] Few studies, however, have compared the properties of late metalloradicals within a group that possess similar geometries and ancillary ligands.[5]

We have recently employed a tripodal, tris(phosphino)silyl ligand, $[SiP^{iPr}_3]H$ ($[SiP^{iPr}_3] = (2\text{-}iPr_2PC_6H_4)_3Si^-$),[6] to stabilize a number of group 8 metalloradicals, including unusual examples of mononuclear ruthenium(I) and osmium(I) complexes.[7] These metalloradicals included a series of dinitrogen complexes of iron(I), ruthenium(I), and osmium(I).[6,7] We herein report on the synthesis and thorough characterization of a related series of isoelectronic PMe_3 adduct complexes of the group 9 metals $\{[SiP^{iPr}_3]M(PMe_3)\}BAr^F_4$ [M = Co (**1**), Rh (**2**), Ir (**3**); BAr^F_4 = tetrakis[3,5-bis(trifluoromethyl)phenyl]borate]. These complexes constitute a rare instance wherein a series of metalloradicals within a group can be isolated and for which their ancillary ligands, oxidation states, spin states, and geometries are conserved.

Entry to the desired d^7, group 9 complexes begins with the dinitrogen complexes $[SiP^{iPr}_3]M(N_2)$ [M = Co (**4**), Rh (**5**), Ir (**6**); Scheme 1]. While complexes **4** and **6** have been reported,[6b] complex **5** has not been previously synthesized. Briefly, **5** is prepared through dehydrodehalogenation of a hydrido chloride complex, $[SiP^{iPr}_3]Rh(H)(Cl)$ (**7**), with MeMgBr in 97% yield. Complex **7**, in turn, is prepared via

Scheme 1. Synthesis of Divalent Group 9 Complexes

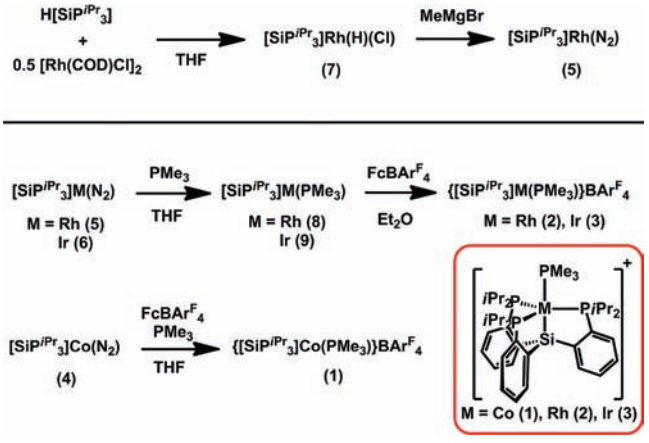

Si–H bond activation by the addition of $[SiP^{iPr}_3]H$ to $[Rh(COD)Cl]_2$ in 87% yield. As previously described for **6**,[6b] complex **5** features a labile N_2 ligand ($\nu_{N_2} = 2159\ cm^{-1}$).

For the rhodium and iridium systems, the addition of excess PMe_3 to complexes **5** and **6** leads to clean substitution to afford the yellow PMe_3 complexes $[SiP^{iPr}_3]M(PMe_3)$ [M = Rh (**8**), Ir (**9**)]. Complexes **8** and **9** reveal reversible oxidation waves at −0.78 and −0.76 V (vs Fc/Fc^+, THF), respectively. Accordingly, the oxidation of **8** and **9** with $FcBAr^F_4$ [Fc = $Fe(C_5H_5)_2$] results in color changes to blue and purple, respectively, and affords the desired 17 e^-, $S = {}^1/_2$ complexes **2** (66%) and **3** (88%).

In contrast to **2** and **3**, the cobalt metalloradical **1** is synthesized by the addition of $FcBAr^F_4$ to a solution containing **4** and excess PMe_3, which yields orange, $S = {}^1/_2$, complex **1** in 58% after workup. Interestingly, the reduction of isolated **1** by $CoCp^*_2$ under an N_2 atmosphere cleanly regenerates the Co^I–N_2 adduct **4** with quantitative loss of PMe_3. Further, complex **4** exhibits no tendency to bind PMe_3 under an atmosphere of N_2. Hence, the apparent stronger preference of Co^I for N_2 over PMe_3 in comparison to the related Rh^I and Ir^I fragments appears to be thermodynamic rather than kinetic in origin.

The solid-state structures of **1**–**3** have been obtained through X-ray diffraction studies (Figure 1 and SI). The geometries about the metal centers are similar, exhibiting distorted trigonal-bipyramidal (TBP) geometries [τ = 0.81 (**1**), 0.75 (**2**), 0.73 (**3**)].[8] This correspondence allows for a

Received: September 23, 2011
Published: December 1, 2011

   dx.doi.org/10.1021/ic202079r | *Inorg. Chem.* 2012, 51, 16–18

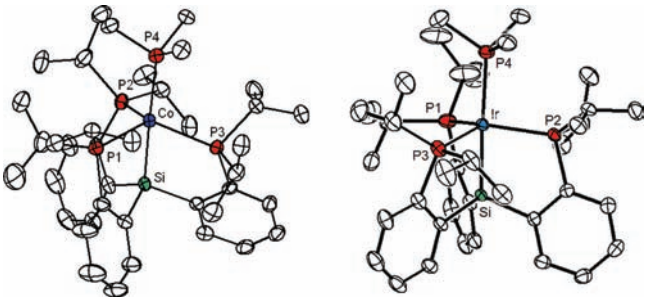

Figure 1. Solid-state structures of $\{[SiP^{iPr}_3]Co(PMe_3)\}\{BAr^F_4\}$ (left) and $\{[SiP^{iPr}_3]Ir(PMe_3)\}\{OTf\}$ (right) at 50% probability. BAr^F_4 and OTf anions, H atoms, and solvent molecules are removed for clarity. For **2**, see SI.

comparison of their chemical and spectroscopic properties. Complexes **1**–**3** each exhibit one P–M–P angle [129.54(4)° (**1**), 131.99(3)° (**2**), 133.51(4)° (**3**)] that is substantially larger than the other two, a feature that was also observed in the solid-state structures of the Ru–N_2 and Os–N_2 metalloradicals, $[SiP^{iPr_3}]M(N_2)$ (M = Ru (**11**), Os(**12**)).[7] The doubly degenerate ^2E ground state of an idealized TBP structure, whereby the $d_{xy}/d_{x^2-y^2}$ orbitals are triply occupied, is subject to Jahn–Teller distortion, consistent with the distorted structural parameters of **1**–**3**.

To assess the metalloradical character of complexes **1**–**3**, their EPR spectra were measured at X-band frequency. Deviations of the isotropic g value from the free-electron value of 2.0023 and the g anisotropy in a frozen solution, Δg ($\Delta g = g_{max} - g_{min}$, where g_{max} and g_{min} are the largest and smallest **g** tensors), have been used as crude indicators in assessing the metalloradical character; large deviations from g = 2.0023 at room temperature and higher values of Δg in a frozen solution typically point to predominant spin on the metal.[1] The room temperature EPR spectra of **2** and **3** are rather featureless (see the SI). For **1** a signal could not be observed at room temperature, likely because of the rapid relaxation induced by the metal center. Complexes **2** and **3** exhibit spectra reminiscent of **11** and **12**, showing broad doublet signals. The splitting pattern indicates strong coupling to one P atom, while coupling to the other P atoms is smaller and unresolved. The observation of asymmetry in the P atoms even at room temperature is due to the faster time scale of the EPR experiment relative to the NMR experiment, where an averaged 3-fold symmetry is suggested. The g values for **2** and **3**, which are 2.100 and 2.145, respectively, are similar to the values of **11** (2.078) and **12** (2.147).

The 77 K X-band EPR spectra taken in 2-MeTHF are shown in Figure 2 and are more revealing. All three spectra are rhombic, with significant anisotropy (Table 1). The Δg values for **1**–**3** are 0.61, 0.18, and 0.33 and, together with the room temperature isotropic g values, suggest significant metalloradical character. While the spectrum of **1** is broad and thus does not show resolvable hyperfine coupling with either the Co or P atoms, the spectra of **2** and **3** exhibit sharp splitting. Both spectra have been simulated by assigning a large hyperfine coupling to one P atom, with smaller coupling to either the P, Rh, or Ir atoms. Large coupling to only one P atom is also seen in the EPR spectra of **11** and **12** at 77 K and is ascribed to coupling to the P atom opposite the largest P–M–P angle that is observed in the solid-state structure. Similar characteristics have been previously proposed for spectroscopically characterized rhodium(II) complexes featuring poly(phosphine) ligands.[9] This large coupling is consistent with the doublet resonance observed at room temperature. The magnitude of this hyperfine coupling, however, is roughly 2-fold greater for **2** and **3** relative to **11** and **12** (Table 1). Note that, although complexes **1**–**3** are metalloradical in character, large hyperfine coupling constants for the P atoms are observed in **2** and **3** because of the large relative gyromagnetic ratio of P compared to Rh (P:Rh = −12.9) and Ir (P:^{191}Ir = 22.6; P:^{193}Ir = 20.9).

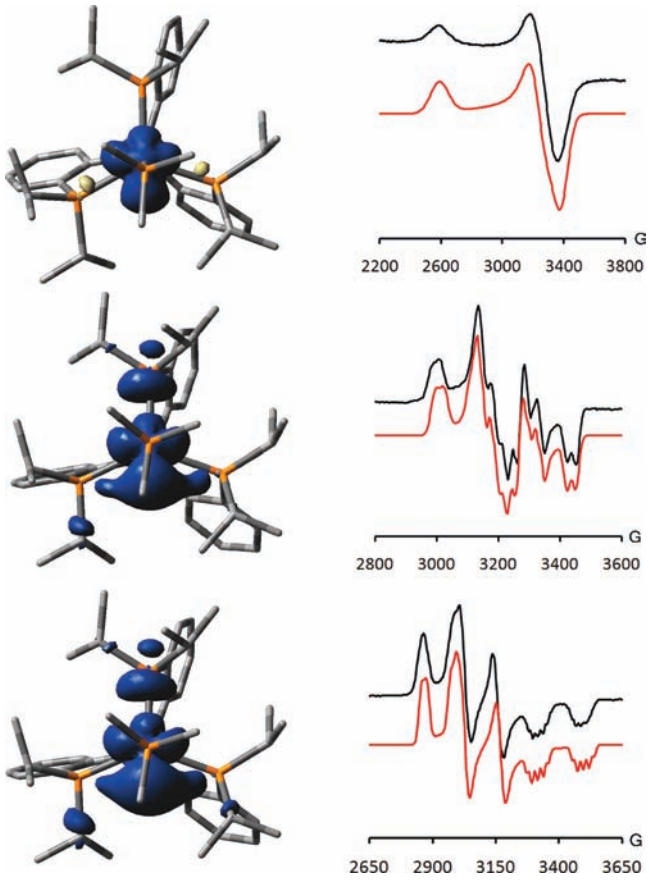

Figure 2. Spin-density plots (left) and 77 K X-band EPR in 2-MeTHF (right) of **1** (top), **2** (center), and **3** (bottom). The spin-density plots are shown looking down the Me_3P–M–Si axis, with the P atom opposite to the largest P–M–P angle at the top. The lower curves in each EPR spectra represent simulations. See the SI for calculation details and full simulation parameters.

Table 1. EPR Parameters for Complexes 1–3, 11, and 12[a]

	Co(**1**)	Rh(**2**)	Ir(**3**)	Ru(**11**)[b]	Os(**12**)[b]
g_x	2.600	2.205	2.300	2.175	2.290
g_y	2.080	2.087	2.170	2.075	2.200
g_z	1.990	2.025	1.975	2.009	1.978
Δg	0.61	0.18	0.33	0.17	0.31
$A(P)_x$	N/A	360	370	220	190
$A(P)_y$	N/A	430	430	230	190
$A(P)_z$	N/A	550	500	250	230

[a]Hyperfine coupling constants are in megahertz and represent values for the largest coupled P atom. For the full set of experimental and simulation parameters, see the SI. [b]Parameters from ref 7.

The conclusions from the EPR data are corroborated by DFT calculations (Table 2). These calculations place Mulliken spin densities of 1.17,[10] 0.74, and 0.73 e^- at the metal centers

dx.doi.org/10.1021/ic202079r | Inorg. Chem. 2012, 51, 16–18

Table 2. Mulliken Spin Densities Obtained from DFT Calculations[a]

	Co(**1**)	Rh(**2**)	Ir(**3**)	Ru(**11**)[b]	Os(**12**)[b]
M	1.167	0.746	0.732	0.836	0.786
P(total)	−0.042	0.233	0.198	0.135	0.129
P_{max}	−0.032	0.170	0.161	0.086	0.073
P_{PMe_3}	−0.025	−0.009	−0.009	−0.009	−0.005

[a] P(total) represents the total spin density from the P atoms of the $[SiP^{iPr}_3]$ scaffold. P_{max} represents the values from the phosphine possessing the greatest spin density. [b] Values from ref 7.

for **1**−**3**, respectively. While small in **1**, delocalization of the spin density onto the phosphines is evident for **2** and **3**, with values of 0.23 and 0.19 e^- distributed among the P atoms of the $[SiP^{iPr}_3]$ scaffold. The greater spin delocalization for **2** and **3** relative to **1** is likely due to the greater covalency of the M−P bonds in the former. In contrast, the apical PMe_3 P atom possesses negligible spin for all three complexes. The small degree of delocalization onto the phosphines in **1** may also explain its featureless 77 K spectrum. Importantly, one P atom in **2** and **3** possesses a notably greater value (0.17 e^- for **2** and 0.16 e^- for **3**) relative to the other two P atoms. This P atom lies opposite the largest P−M−P angle in the equatorial plane of these complexes, and this observation is consistent with the EPR simulations that assign a large hyperfine coupling to this atom. The numbers are roughly double the value observed for the P atom with the largest spin densities in **11** (0.09 e^-) and **12** (0.07e^-) and suggest a greater spin delocalization for the group 9 complexes, in agreement with the EPR parameters (Table 1). Thus, both the EPR simulations and DFT calculations are qualitatively consistent and point to the metalloradical character for **1**−**3**, with a greater degree of spin leakage for the second- and third-row derivatives **2** and **3**.

The frontier orbitals of complexes **1**−**3** are also of interest. For all three complexes, the LUMO is ligand-based and the SOMO and SOMO−1 are of $d_{xy}/d_{x^2-y^2}$ parentage (see the SI). While the LUMO and SOMO energy difference remains relatively constant, the SOMO and SOMO−1 energy difference increases from **1** to **3**, from 5.7 to 16.9 kcal/mol. Observation of the largest g anisotropy in complex **1**, despite the smaller spin−orbit coupling constant for Co relative to Rh and Ir, is thus not only due to the greater spin density on the metal center, as suggested by DFT calculations, but also of greater admixture of the SOMO with filled orbitals.

In conclusion, a series of d^7 complexes of group 9 metals has been synthesized and thoroughly characterized. The electronic structures of these complexes have been probed through EPR spectroscopy and DFT calculations, and these results suggest metalloradical character. Comparison of the complexes within the series indicates greater spin delocalization onto the phosphines for Rh and Ir relative to Co. Further, a comparison of the rhodium and iridium complexes, **2** and **3**, with their isoelectronic group 8 analogues, complexes **11** and **12**, points to similar electronic structures for the two sets of complexes but with increased spin delocalization onto the phosphines for **2** and **3**. The degree of covalency observed in the M−P bonds in complexes **2**, **3**, **11**, and **12** may explain the unusual stability of these second- and third-row low-valent metalloradicals, for which few are isolable and structurally characterized.[11]

■ ASSOCIATED CONTENT

Ⓢ Supporting Information

X-ray crystallographic data in CIF format, synthetic and spectroscopic details and data, computational details, and solid-state structures. This material is available free of charge via the Internet at http://pubs.acs.org.

■ AUTHOR INFORMATION

Corresponding Author

*E-mail: jpeters@caltech.edu.

■ ACKNOWLEDGMENTS

This work was supported by the NSF (Grant CHE-0750234). Charlene Tsay and Larry Henling are acknowledged for crystallographic assistance.

■ REFERENCES

(1) de Bruin, B.; Hetterscheid, D. G. H.; Koekkoek, A. J. J.; Grützmacher, H. *Prog. Inorg. Chem.* **2007**, *55*, 247.

(2) Cui, W.; Li, S.; Wayland, B. B. *J. Organomet. Chem.* **2007**, *692*, 3198.

(3) (a) Sherry, A. E.; Wayland, B. B. *J. Am. Chem. Soc.* **1990**, *112*, 1259. (b) Wayland, B. B.; Ba, S.; Sherry, A. E. *J. Am. Chem. Soc.* **1991**, *113*, 5305.

(4) Poli, R. *Angew. Chem., Int. Ed.* **2010**, *49*, 2. (b) Wayland, B. B.; Ba, S.; Sherry, A. E. *J. Am. Chem. Soc.* **1991**, *113*, 5305.

(5) (a) Palmer, J. H.; Mahammed, A.; Lancaster, K. M.; Gross, Z.; Gray, H. B. *Inorg. Chem.* **2009**, *48*, 9308. (b) Zhai, H.; Bunn, A.; Wayland, B. *Chem. Commun.* **2001**, 1294. (c) Deblon, S.; Liesum, L.; Harmer, J.; Schönberg, H.; Schweiger, A.; Grützmacher, H. *Chem.—Eur. J.* **2002**, *8*, 601.

(6) (a) Mankad, N. P.; Whited, M. T.; Peters, J. C. *Angew. Chem., Int. Ed.* **2007**, *129*, 5768. (b) Whited, M. T.; Mankad, N. P.; Lee, Y.; Oblad, P. F.; Peters, J. C. *Inorg. Chem.* **2009**, *48*, 2507.

(7) Takaoka, A.; Gerber, L. C. H.; Peters, J. C. *Angew. Chem., Int. Ed.* **2010**, *49*, 4088.

(8) $\tau = (b - a)/60$, where b and a represent the two largest angles. See: Addison, A. W.; Rao, T. N.; Van Rijn, J. J.; Verschoor, G. C. *J. Chem. Soc., Dalton Trans.* **1984**, 1349.

(9) Bianchini, C.; Meli, A.; Peruzzini, M.; Vacca, A. *Organometallics* **1990**, *9*, 360.

(10) Some negative spin due to spin polarization is observed on the silicon (−0.09 e^-).

(11) Representative examples: (a) Danopoulos, A. A.; Wilkinson, G.; Hussain-Bates, B.; Hursthouse, M. B. *J. Chem. Soc., Dalton Trans.* **1992**, 3165. (b) García, M. P.; Jiménez, M. V.; Oro, L. A.; Lahoz, F. J. *Organometallics* **1993**, *12*, 4660. (c) García, M. P.; Jiménez, M. V.; Oro, L. A.; Lahoz, F. J.; Casas, J. M.; Alonso, P. J. *Organometallics* **1993**, *12*, 3257. (d) Dunbar, K. R.; Haefner, S. C. *Organometallics* **1992**, *11*, 1431. (e) Connely, N. G.; Emslie, D. J. H.; Metz, B.; Orpen, A. G.; Quayle, M. J. *Chem. Commun.* **1996**, 2289. (f) Dzik, W. I.; Arruga, L. F.; Siegler, M. A.; Spek, A. L.; Reek, J. N. H.; de Bruin, B. *Organometallics* **2011**, *30*, 1902. (g) Connely, N. G.; Emslie, D. J. H.; Metz, B.; Orpen, A. G.; Quayle, M. J. *Chem. Commun.* **1996**, 2289.